Title	β^- decay of $T_z = +\frac{11}{2}$ isotopes ^{37}Al and ^{39}Si; Understanding Gamow-Teller strength distribution in neutron-rich nuclei
Author(s)	Abromeit B., Tripathi V., Crawford H. L., Liddick S. N., Yoshida Sota, Utsuno Yutaka, Bender P. C., Crider B. P., Dungan R., Fallon P., Kravvaris K., Larson N., Lubna R. S., Otsuka Takaharu, Prokop C. J., Richard A. L., Shimizu Noritaka, Tabor S. L., Volya A.
Citation	Physical Review C,100(1),p.014323_1-014323_14
Text Version	Published Journal Article
URL	https://jopss.jaea.go.jp/search/servlet/search?5066422
DOI	https://doi.org/10.1103/PhysRevC.100.014323
Right	

β^- decay of $T_z = +\frac{11}{2}$ isotopes ^{37}Al and ^{39}Si: Understanding Gamow-Teller strength distribution in neutron-rich nuclei

B. Abromeit,[1] Vandana Tripathi,[1,*] H. L. Crawford,[2] S. N. Liddick,[3,4] S. Yoshida,[5] Y. Utsuno,[6,7] P. C. Bender,[4,†] B. P. Crider,[4,‡] R. Dungan,[1] P. Fallon,[2] K. Kravvaris,[1] N. Larson,[3,4] R. S. Lubna,[1] T. Otsuka,[5,4,8] C. J. Prokop,[3,4] A. L. Richard,[4] N. Shimizu,[7] S. L. Tabor,[1] and A. Volya[1]

[1]*Department of Physics, Florida State University, Tallahassee, Florida 32306, USA*
[2]*Nuclear Science Division, Lawrence Berkeley National Laboratory, Berkeley, California 94720, USA*
[3]*Department of Chemistry, Michigan State University, East Lansing, Michigan 48824, USA*
[4]*National Superconducting Cyclotron Laboratory, Michigan State University, East Lansing, Michigan 48824, USA*
[5]*Department of Physics, University of Tokyo, Hongo, Bunkyo-ku, Tokyo 113-0033, Japan*
[6]*Advanced Science Research Center, Japan Atomic Energy Agency, Tokai, Ibaraki 319-1195, Japan*
[7]*Center for Nuclear Study, University of Tokyo, Hongo, Bunkyo-ku, Tokyo 113-0033, Japan*
[8]*Instituut voor Kern-en Stralingsfysica, Katholieke Universiteit Leuven, B-3001 Leuven, Belgium*

(Received 1 May 2019; published 29 July 2019)

β^- decay of $T_z = +\frac{11}{2}$ nuclei ^{37}Al and ^{39}Si was studied to obtain information about excited states in the daughter and granddaughter nuclei. New information on excited states has been obtained for ^{37,39}P, whereas level schemes for ^{37}Si and ^{37,39}S were confirmed and expanded on as compared to the most recent investigations. For the nuclei studied, the valence proton and neutron occupy different major shells with opposite parities, hence, the β^- decay preferentially and primarily populates core-excited $1p1h$ intruder states with a parity opposite to the ground state of the daughter nucleus. These low-lying intruder states shed light on the $N = 20$ shell gap and its evolution with neutron number. The β^- decay of very neutron-rich nuclei also illustrates how the Gamow-Teller (GT) strength distribution changes with neutron excess. Comparing β^- decay of ^{37,39}Si presented here with ^{38,40}Si from a previous study, we clearly see an even-odd effect in the GT strength distribution with the decay from even-even nuclei showing strong low-lying strength whereas for the odd A being very fragmented. Configuration interaction shell-model calculations with the state-of-art SDPFSDG-MU effective interaction were performed to understand the structure of the $1p1h$ states and explore the GT strength distribution.

DOI: 10.1103/PhysRevC.100.014323

I. INTRODUCTION

β-delayed γ-ray spectroscopy is a powerful probe for nuclear structure studies and is especially invaluable for those nuclei farthest from stability where low production rates make other experiments difficult [1]. Highly selective allowed β decay leads to a definitive range in spin and parity for excited states in the daughter nucleus provided the spin and parity of the parent is known [2]. The good characterization of the final states allows for useful comparisons with theoretical predictions. β-decay studies also provide other important information, such as decay lifetimes and β-delayed neutron- and proton-emission probabilities which are important inputs to network calculations of the astrophysical rapid neutron capture and rapid proton capture processes.

Although the β-decay process is quite well understood, in general, there are open questions when it comes to the decay of nuclei with neutron excess beyond one major shell. Here, as the neutrons near the Fermi energy occupy orbitals in a different oscillator shell than the protons, Gamow-Teller (GT) transitions likely involve the conversion of deeply bound neutrons. Recently, in the decay of neutron-rich zinc and gallium isotopes near ^{78}Ni [3,4], GT transitions were shown to populate high-lying core-excited states in the daughter nuclei. On the other hand, in our investigation of ^{38,40}Si decay [5], based on the allowed β^- decay, 1^+ states were clearly identified in both ^{38,40}P's which lie at relatively low excitation energies of $\sim$2 MeV. Also, there is experimental evidence of γ decay from states populated above the neutron emission threshold in the daughter nucleus [6]. It is proposed that these are $E1$ transitions from coherent dipole oscillations likely caused by an abrupt change in the nuclear density of the decaying parent due to the transformation of a deeply bound neutron. This could also be a possible mechanism explaining the large β feeding to low-energy states previously attributed to first forbidden (FF) transitions [4]: The GT fed neutron unbound resonance states decay by $E1$ transitions which are unobserved in most discrete spectroscopy experiments.

In this paper, we report on the β^- decay of two very neutron-rich isotopes, namely, ^{37}Al and ^{39}Si with $T_z = \frac{11}{2}$ to

*Corresponding author: tripathi.vandana@gmail.com
†Present address: Department of Physics, University of Massachusetts Lowell, Lowell, Massachusetts 01854, USA.
‡Present address: Department of Physics and Astronomy, Mississippi State University, Mississippi State, Mississippi 39762, USA.

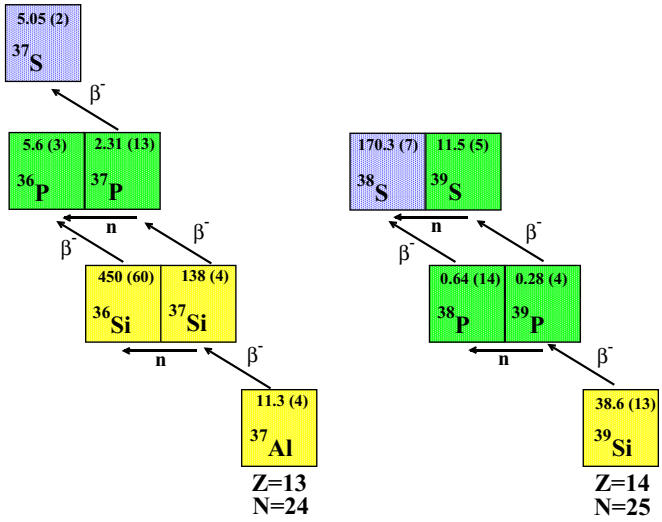

FIG. 1. The decay chain showing the half-lives of β decay and β-delayed neutron emission daughters for the two neutron-rich isotopes reported in this paper, namely, ^{37}Al and ^{39}Si (both $T_z = +11/2$). The half-lives ($T_{1/2}$) of ^{37}Al and ^{37,39}Si are from this paper, whereas the rest are from National Nuclear Data Center (NNDC) [17]. Half-lives in milliseconds marked in yellow, seconds in green and minutes in purple boxes.

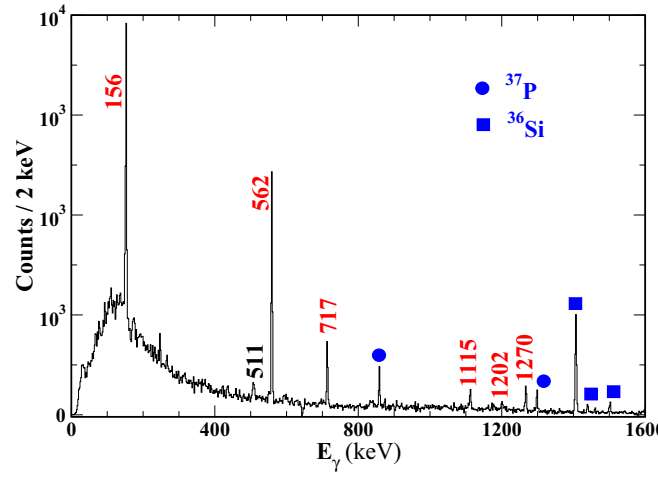

FIG. 2. β-delayed γ spectrum observed for 50 ms after an initial ^{37}Al implant. Transitions in the daughter nucleus ^{37}Si are indicated by their energies in keV. γ transitions in ^{36}Si populated in β-delayed one-neutron emission as well those from granddaughter ^{37}P are also highlighted.

further explore the distribution of GT strengths. The β^- decay also allowed us to study the excited states in the daughter and granddaughter nuclei through delayed γ-ray spectroscopy (Fig. 1). The β^- decay of ^{37}Al was studied recently [7], and we were able, in the present paper, to confirm the observed level scheme and determine the log ft values precisely. This is the first study of the β^- decay of ^{37,39}Si leading to excited states in the respective phosphorus isotopes. Although a few low-lying positive-parity states have been identified in both ^{37,39}P's previously [8,9], negative-parity intruder states were observed here for the first time. For the decay of exotic odd-A Si isotopes presented here, the Gamow-Teller transition strength [B(GT)] is very fragmented with no strong population of states beyond the low-lying positive-parity states which are likely fed indirectly. This is in contrast to the decay of the even-A Si isotopes as mentioned before. Following the decay chain, we were able to establish the level schemes of ^{37,39}S via the decay of the P isobars. Unlike the β decay of the Si isotopes here, we see strong population of specific states in both cases. The experimental results are interpreted within configuration interaction shell-model (SM) calculations using the SDPFSDG-MU interaction [10,11].

II. EXPERIMENTAL DETAILS

The experiment to investigate the β^- decay of ^{37}Al and ^{39}Si was carried out at the National Superconducting Cyclotron Laboratory (NSCL) [12] at Michigan State University. A 140-MeV/u ^{48}Ca primary beam was fragmented in a Be target of thickness 775 mg/cm^2 at the target position of the A1900 fragment separator [13] to produce the nuclei of interest. A wedge-shaped Al degrader (45 mg/cm^2) was used at the intermediate dispersive image of A1900 for further energy dispersion. With a full momentum acceptance of 5.08% of the A1900, a cocktail beam centered around ^{36}Mg was obtained at the focal plane of the A1900 which was transported to the β-counting system (BCS). The BCS is centered around a 1-cm-thick 16 × 16 segmented planar germanium double-sided strip detector (GeDSSD) [14], which recorded the time and position of implants (GeV energy depositions) as well as subsequent decays (keV to MeV energy depositions) by using dual-gain preamplifiers. The implant rate was kept low, around 100 Hz, so as to maximize the efficiency of correlating

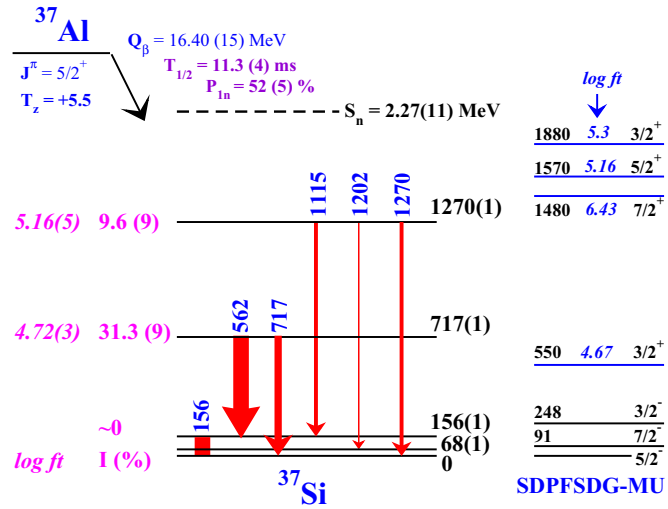

FIG. 3. Partial level scheme of ^{37}Si as established in the present β^- decay of ^{37}Al, similar to the most recent work [7]. The measured half-life and P_{1n} value are also shown. The measured absolute branching, half-life, and Q_{β^-} [17] were used to calculate the log ft values [19] of the excited states at 717 and 1270 keV. Shell-model calculations (see the text for details) employing the SDPFSDG-MU interaction [10,11] are also shown alongside.

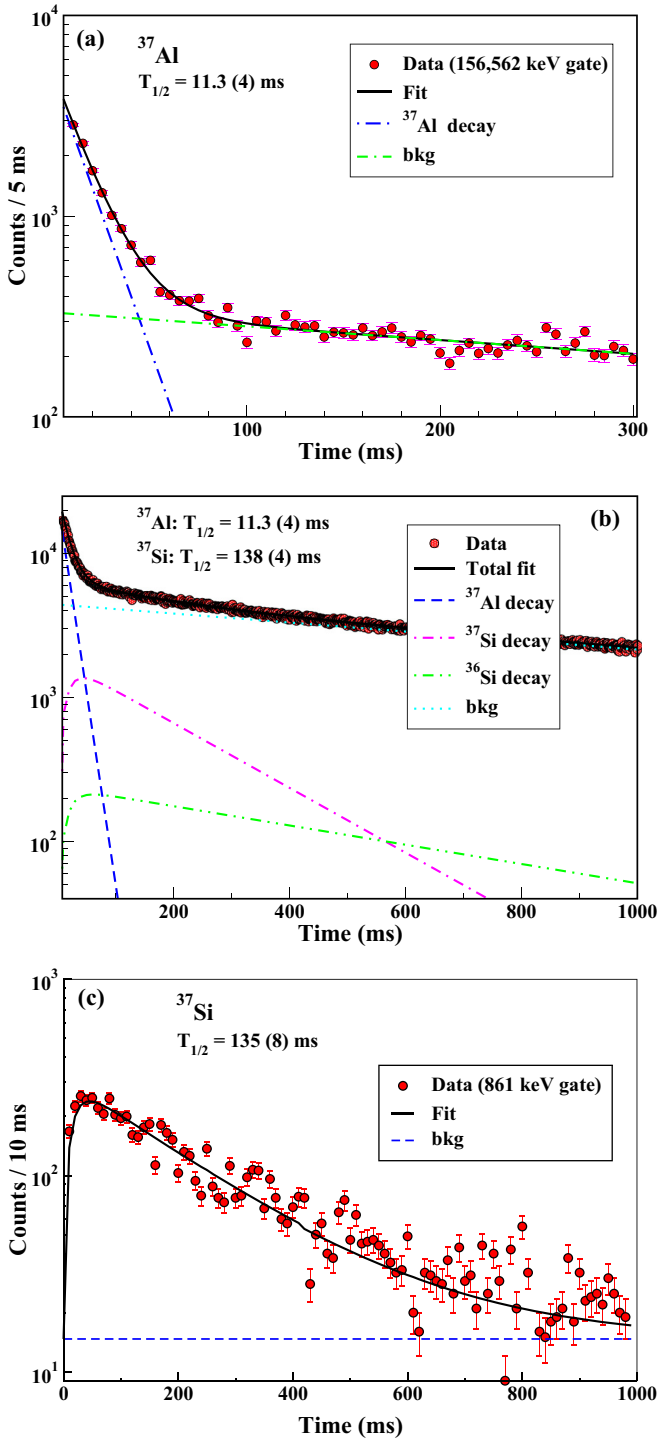

FIG. 4. (a) Decay curve for ^{37}Al implants in coincidence with γ transitions in ^{37}Si (156 and 562 keV). The fit is an exponential with two free parameters and a background. (b) Decay curve derived for ^{37}Al from β-correlated implants within the same pixel for 1000 ms along with the fit used to extract half-life and the initial activity. The components of the fit are as follows: (i) exponential decay of parent ^{37}Al, (ii) exponential growth and decay of daughter nuclei ^{37}Si (β), ^{36}Si (β-n), and (iii) exponential background. Known half-lives were used for the daughter nuclides [17]. (c) Decay curve for ^{37}Al implants in coincidence with γ transitions in granddaughter ^{37}P, displaying the growth and decay of ^{37}Si.

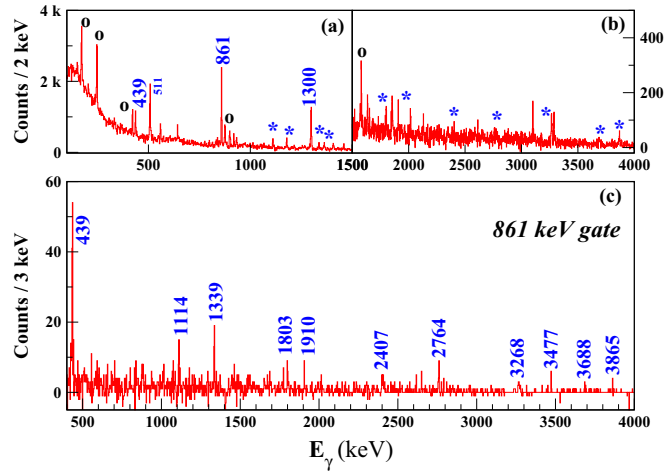

FIG. 5. (a) and (b) represent β-delayed γ spectrum observed for the time-interval 50–500 ms after an ^{37}Al implant with background subtraction. (The first 50 ms are dominated by transitions in ^{37}Si.) The two strong transitions at 861 and 1300 keV were already known to belong to ^{37}P. Transitions marked with **o** are deexcitations in ^{36}P, whereas those with ∗ are new candidates for ^{37}P. Precise energies of the γ transitions are listed in Table I. (c) Transitions seen in coincidence with the 861-keV transition in ^{37}P.

the implanted ion with the decay products. Three Si PIN detectors placed upstream of the GeDSSD provided the energy loss and time-of-flight information (along with the scintillator at the intermediate dispersive image of the A1900) for particle identification of the incoming implants. The GeDSSD was surrounded by 16 detectors of the segmented germanium array [15] to record the β-delayed γ rays with an efficiency of about 3.5% at 1 MeV. Part of the results from this experiment

TABLE I. γ-ray energies in keV along with the measured relative intensities for the transitions proposed to be in ^{37}P and ^{39}P populated in the β decay of the respective Si isobar.

^{37}P		^{39}P	
E_γ	I_γ	E_γ	I_γ
438.7(5)	30(5)	355.1(5)	84(3)
860.9(5)	100	616.8(10)	10(1)
1114.3		973.1(5)	100
1180.6(10)	20(3)	1200(2)	24(3)
1300.1(10)	95(5)	1218.5(10)	15(3)
1338.7(10)	14(2)	1244(2)	18(2)
1364.5(10)	14(2)	1550.3(10)	25(3)
1802.5(15)	13(3)	1817.5(10)	9(2)
1910.0(10)	14(2)	1836.9(10)	19(2)
2406.5(20)	4(1)	2004(2)	4(1)
2763.9(20)	9(3)	2233.4(15)	11(2)
3005.0(30)	<1	2267.7(20)	3(1)
3268.4(25)	30(8)	2812(2)	10(2)
3477.3(25)	2(1)	3173(2)	9(2)
3688.3(25)	8(3)	3189.2(20)	14(3)
3864.8(25)	8(3)	3427.8(20)	12(3)

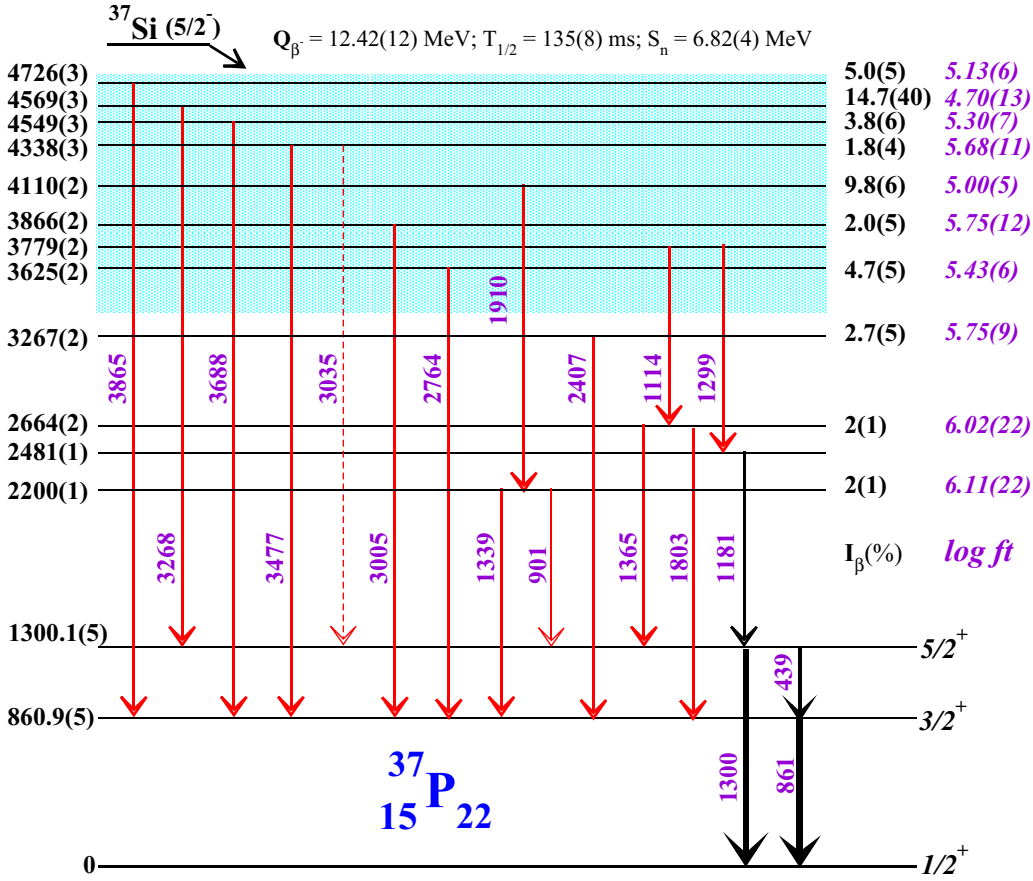

FIG. 6. Partial level scheme for ^{37}P as obtained in the present paper. Transitions shown in black were previously known whereas the new additions from this paper are displayed in red. Measured apparent absolute β branching and log ft values are also indicated. The 1300-keV state is assumed to be a doublet, and the 1114-keV state overlaps with the 1115-keV transition in ^{37}Si (Fig. 2), and hence, their intensities could not be extracted. log ft values for the lowest $3/2^+$ and $5/2^+$ states are not shown as they are not expected to be populated directly in the β decay of ^{37}Si which has ground-state $J^\pi = 5/2^-$. The shaded box indicated the states which are presumed to be directly populated in the β decay of ^{37}Si and are candidates for intruders states with negative parity.

(β^- decay of ^{38,40}Si) have been published [5], and more details on the analysis are given there.

III. RESULTS

A. Decay of ^{37}Al

Similar to the recent study of ^{37}Al decay [7], the β-delayed γ spectrum showed clear γ transitions at 156, 562, 717, 1115, 1202, and 1270 keV in a 50-ms time-correlation window all of which can be attributed to the daughter nucleus ^{37}Si (Fig. 2). The relative intensities of the γ transitions as observed are 100, 92, 34, 16, 7, and 17%, respectively, in excellent agreement with the literature values [7]. The 562- and 1115-keV transitions are in coincidence with the 156-keV γ resulting in states at 717 and 1270 keV, respectively, which also have a direct ground-state decay branch. The level scheme of ^{37}Si as inferred from this paper is shown in Fig. 3 and is identical to Ref. [7]. The decay from the 68-keV state was not observed in our data likely due to attenuation in the implant detector. A strong peak at 1408 keV from the decay of the 2^+ state in ^{36}Si was also observed in the delayed spectrum (Fig. 2) signaling a strong β^--delayed one-neutron emission branch.

The time differences between an implant (^{37}Al in this case) and the β particles detected in the same pixel were histogrammed to generate the decay curve which was used to extract the half-life of the implant as well as the initial activity. The decay curve in coincidence with the two strongest γ transitions in ^{37}Si, namely, 156 and 562 keV is shown in Fig. 4(a). A fit using a simple exponential function with two parameters for the ^{37}Al decay and a background component gave a half-life of 11.3(4) ms, in excellent agreement with Ref. [7]. The decay curve without requiring a coincidence with the γ transitions is shown in Fig. 4(b). Here, the decay of ^{37}Al, the daughter ^{37}Si, and the β-delayed neutron emission daughter ^{36}Si were taken into account simultaneously in the 1000-ms time window. The decay curve was fit using the Bateman equations along with an exponential background [16] to account for longer-lived activity. For the fit, the half-life of ^{37}Al and ^{36}Si (Fig. 1) were kept fixed, while varying the activity of ^{37}Al, ^{37,36}Si, and the half-life of ^{37}Si. The half-life of ^{37}Si was previously measured to be 90(60) ms [17] and 150(7) ms [18]. The fit described above yielded the half-life of ^{37}Si to be 138(4) ms. This half-life of ^{37}Si was confirmed by γ coincidence with the 861-keV transition in ^{37}P

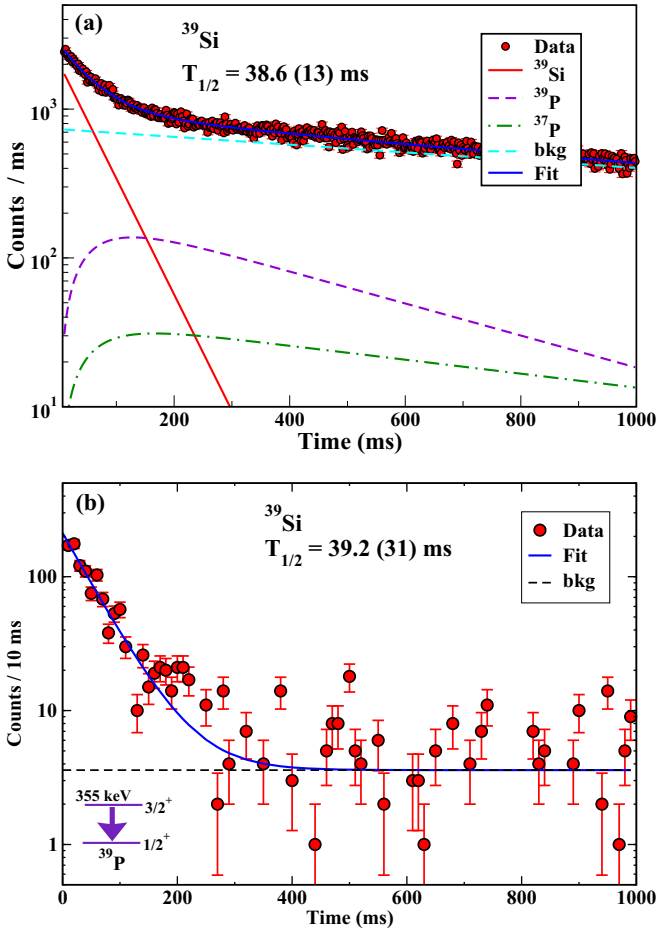

FIG. 7. (a) Decay curve derived for ^{39}Si from β-correlated implants within the same pixel for 1000 ms along with the fit used to extract half-life and the initial activity. The components of the fit are as follows: (i) exponential decay of the parent ^{39}Si, (ii) exponential growth and decay of the daughter nuclei ^{39}P (β), ^{38}P (β-n), and (iii) exponential background. Known half-lives were used for the daughter nuclides [17]. (b) Decay curve of ^{39}Si in coincidence with the lowest 355-keV transition in ^{39}P, fitted with an exponential and a constant background.

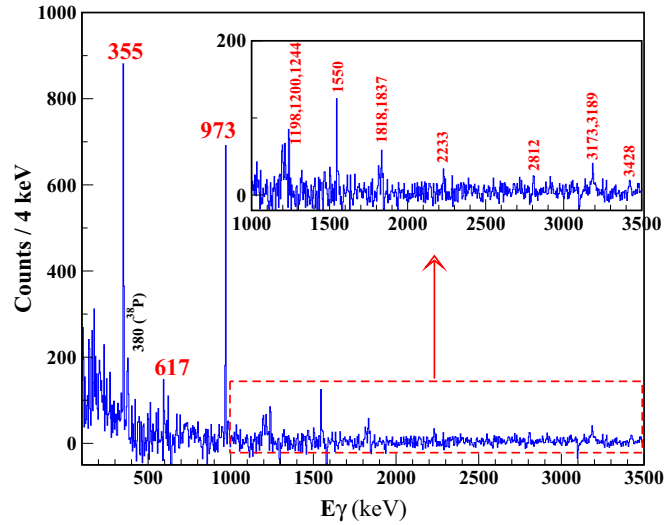

FIG. 8. β-delayed γ spectrum observed for 50 ms after a ^{39}Si implant. The γ transitions in the daughter nucleus ^{39}P are indicated by their energies. The 380-keV transition likely arises from the β-delayed neutron daughter ^{38}P. The inset shows the region from 1 to 3.5 MeV with an expanded y scale.

(discussed in the next section). The decay curve in coincidence with the 861-keV transition is shown in Fig. 4(c) and was fit taking the growth and decay of ^{37}Si into account along with a constant background to give a half-life of 135(8) ms for ^{37}Si.

The total number of implants derived from the decay curve (3.76×10^5 ^{37}Al implants) was used to calculate the absolute β feeding to the states in ^{37}Si and further the log ft values [19]. The measured half-life of 11.3(4) ms was used along with the Q_{β^-} value of 16.40(15) MeV [17]. The absolute branching and log ft values are indicated in Fig. 3 and are consistent with the limits that were proposed in the previous work [7]. As the ground states of ^{37}Al and ^{37}Si have positive and negative parities, respectively (due to the last unpaired nucleon being in the sd and fp orbitals), zero feeding to the ground state was assumed. With this assumption, the branching to the observed bound states observed is about 42%. In the previous work, the β-delayed neutron emission probability (P_{1n}) was proposed to be >29(3)%. To get a better estimate of the neutron emission probability, we followed the β decay of the β-1n daughter ^{36}Si to ^{36}P and used the known absolute branching ratios of the γ rays in ^{36}P [20] to estimate the P_{1n} value to be 52(5)%, which is quite high but consistent with an earlier work [21]. From our paper, we see that about a third of the β branching goes to the excited state at 717(1) keV likely to be a $3/2^+$ state by comparing with shell-model calculations (to be discussed later) which would be consistent with an allowed GT transition from the $5/2^+$ ground state of ^{37}Al.

B. Decay of ^{37}Si

The ^{37}Al ions which were implanted in the GeDSSD within a very short time decay to ^{37}Si which, in turn, β^- decays to ^{37}P. The isotope ^{37}Si with $Z = 14$ and $N = 23$ has a negative parity for its ground state due to the odd neutron in the fp shell, and the shell model predicts a spin and parity of $5/2^-$. On the other hand, the daughter ^{37}P ($Z = 15$, $N = 22$) has a $J^\pi = 1/2^+$ for the ground state due to the unpaired proton in the $1s_{1/2}$ orbital. The allowed GT transitions will, thus, populate negative-parity states in the spin range of 3/2 to 7/2 in ^{37}P following the rules of no parity change and spin change of up to 1 from the ground state of the parent. As ^{37}P has an even number of neutrons ($N = 22$) in the fp shell, these will clearly be excited states created by promoting one nucleon up from the sd to the fp shell ($1p1h$ states). The β^- decay of ^{37}Si will, thus, likely involve the conversion of a core sd-shell neutron to a proton in the sd shell creating a $1p1h$ state in the daughter.

The β-delayed γ spectrum for the time-interval 50–500 ms from the initial ^{37}Al implant is shown in Figs. 5(a) and 5(b). The first 50 ms are dominated by the transitions from the decay of ^{37}Al as discussed in the previous section. Some of

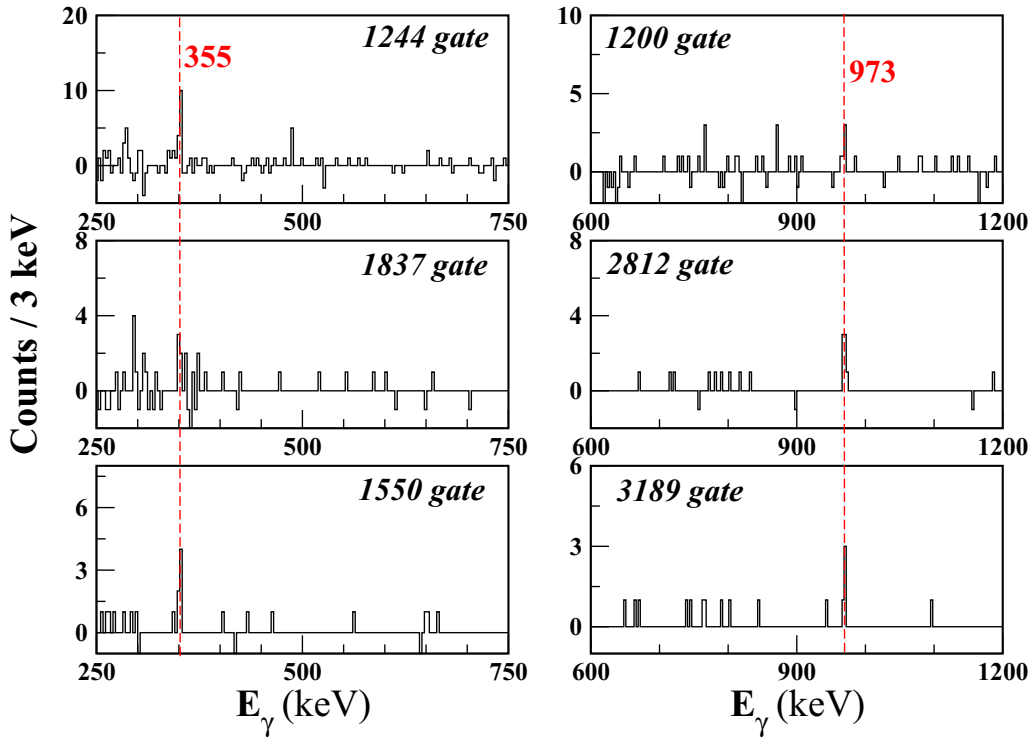

FIG. 9. Coincidences with the 355- and 973-keV transitions in ^{39}P which help build the level scheme.

the strongest lines that were observed belong to ^{36}P following ^{36}Si (the β-n daughter of ^{37}Al) decay. The 861- and the 1300-keV transitions which are decays from the two low-lying positive-parity states in ^{37}P ($3/2^+$ and $5/2^+$, respectively) [8] also stand out. They are probably not populated directly in the β^- decay of ^{37}Si. Apart from that, a number of weak transitions is seen which can be attributed to ^{37}P. Many of these transitions are seen in coincidence with the 861-keV transition Fig. 5(c) and account for most of the feeding to the 861-keV level. Fewer γ decays feed the 1300-keV state, on the other hand. The intensities of the γ transitions proposed to be in ^{37}P, relative to the strongest 861-keV transition, are given in Table I.

Based on the limited coincidences, energy differences and intensity balance a partial level scheme for ^{37}P has been proposed as shown in Fig. 6. Further investigation is needed to confirm the level scheme as the statistics were limited in this experiment. Apparent absolute β feeding to the excited states in ^{37}P was obtained using the initial activity of ^{37}Al corrected for delayed neutron emission. Furthermore, log ft values were calculated using the measured $T_{1/2} = 135(8)$-ms and Q_{β^-} values of 12.42(12) MeV [17]. For the lowest states at 861 and 1300 keV, there is an unexpected large apparent feeding (9% and 17%, respectively), which could result from the pandemonium effect [22]. The proposed level scheme highlights that the β^--decay strength distribution in this case is very fragmented with no single bound state being strongly populated, which is quite different from that seen in the decay of ^{37}Al as discussed previously. Also, as fewer γ transitions observed feed into the 1300-keV state, there is a large net feeding to this state observed, which might seem to suggest that the FF transition is stronger than expected. Conversely, the contributions of FF transitions were explored in Ref. [11] and were found not to be significant. Although the FF transition to the first $5/2^+$ in ^{37}P is calculated to be strong on a relative scale, what we observe is likely due to missing transitions from high-lying states which could even be neutron unbound as has been suggested in Ref. [6]. As the Q_{β^-} is quite large compared to the neutron separation energy (S_n) in the daughter nucleus, we expect to see population of neutron unbound states in the β^- decay. These unbound states, decaying through emission of a neutron with $l = 0$ will populate either low-lying negative states in ^{36}P or the ground state which likely has $J^\pi = 4^-$. In the present case, we cannot use the γ transitions in ^{36}P to infer about delayed neutron emission from ^{37}Si as ^{36}Si is also in the decay chain where also β decays to ^{36}P (Fig. 1) and the intensities observed are consistent with that route. The other possibilities are that the neutron emission populates the ground state or there could be competition with γ emission which could be feeding the 1300-keV state by high-energy γ rays that were not observed in the present measurement.

C. Decay of ^{39}Si

The half-life of ^{39}Si and the initial activity were extracted by fitting the decay curve following the decay chain as shown in Fig. 7(a). The half-life obtained is 38.6 (13) ms which was further confirmed by gating on the known γ transition in the daughter ^{39}P, namely, 355 keV which deexcites the first excited state [Fig. 7(b)]. This gave a value of 39.2 (31) ms for the half-life of ^{39}Si; our values are somewhat smaller than the

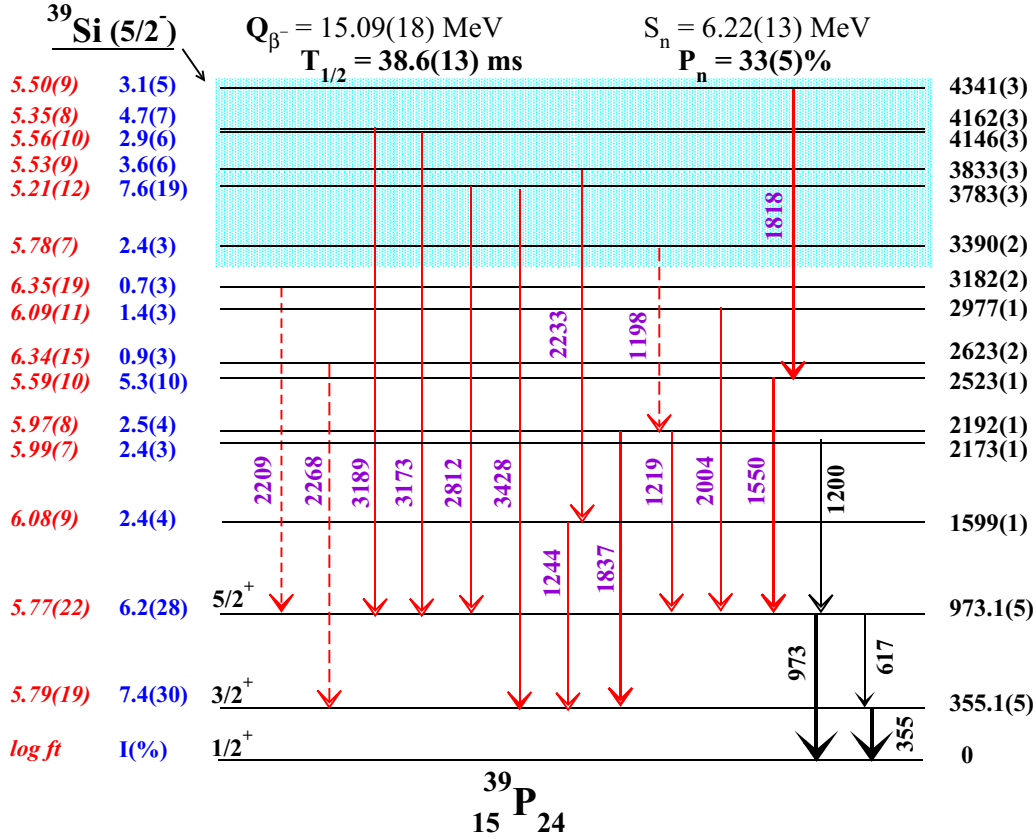

FIG. 10. Partial level scheme of ^{39}P as established in the present β^- decay of ^{39}Si. The measured absolute branching, half-life, and Q_{β^-} [17] were used to calculate the log ft values [19]. The shaded box indicates the states which are presumed to be directly populated in the β decay of ^{39}Si and are candidates for intruders states with negative parity.

previously published value of 47.5(20) ms [17] but in good agreement with shell-model calculations discussed later.

The β^--delayed γ spectrum collected for 50 ms after the ^{39}Si implant is shown in Fig. 8, and much like ^{37}Si, the two strongest transitions seen, 355 and 973 keV, are the decays from the two lowest excited states both with known positive parity ($3/2^+$ and $5/2^+$, respectively). A number of weak transitions can be seen as shown in the inset of Fig. 8 which is in coincidence with either the 355- or the 973-keV transitions. The intensities of the γ transitions in ^{39}P normalized to the strongest 973 keV transition are given in Table I. Although not overwhelming tentative coincidences, shown in Fig. 9, allowed us to construct a partial level scheme of ^{39}Si shown in Fig. 10. Using the total number of the ^{39}Si implants and half-life extracted from the decay curve along with the Q_{β^-}, log ft values have been obtained. They should be treated as limits to allow for uncertainties in the level scheme.

The β-delayed neutron emission is expected to be strong based on the large Q_{β^-} of 15.09(18) MeV and a low S_n of 6.22(13) MeV in ^{39}P. However, no strong transitions from ^{38}P were observed in the delayed γ spectrum, only a very weak 380 keV which is likely the $4^- \rightarrow 2^-$ transition in ^{38}P [23]. The neutron emission likely then goes to the ground state of ^{38}P which then decays with a half-life of 0.64(14) s to ^{38}S. In the β-delayed γ spectrum observed for 5 s from the initial implant, we see the 1292-keV transition from ^{38}S which has an absolute branching of ≈0.8 from Ref. [20]. Using that branching ratio, we obtain a one-neutron emission probability (P_{1n}) of 33(3)%. This value is consistent with the systematics in nearby Si isotopes: In our recent work [5], we quoted 25(10)% and 38(5)% for ^{38}Si and ^{40}Si, respectively. It is also consistent with the branching to the bound states observed.

D. Decay of ^{37,39}P

We were able to observe γ transitions in the daughter nuclei of ^{37,39}P decay by following the decay chains presented above. The β decays of ^{37,39}P have been studied [20,24] before, although the observed γ transitions were not placed in the level scheme due to lack of coincidence data. We were able to observe coincidences between the observed γ transitions for ^{37}P decay to ^{37}S as can be seen in Fig. 11(a). The strongest 646-keV γ transition shows clear coincidence with the γ transitions at 751, 1583, 2102, 2254 keV, and so they are all proposed to feed the 646-keV state. Thus, the 646-keV state is not being fed directly in the β^- decay which is consistent with its $J^\pi = 3/2^-$ assignment as shown in Fig. 12. Based on the relative intensities in Ref. [20], the state at 2229 keV has the strongest direct β feeding and is likely a $1/2^+$ state as the

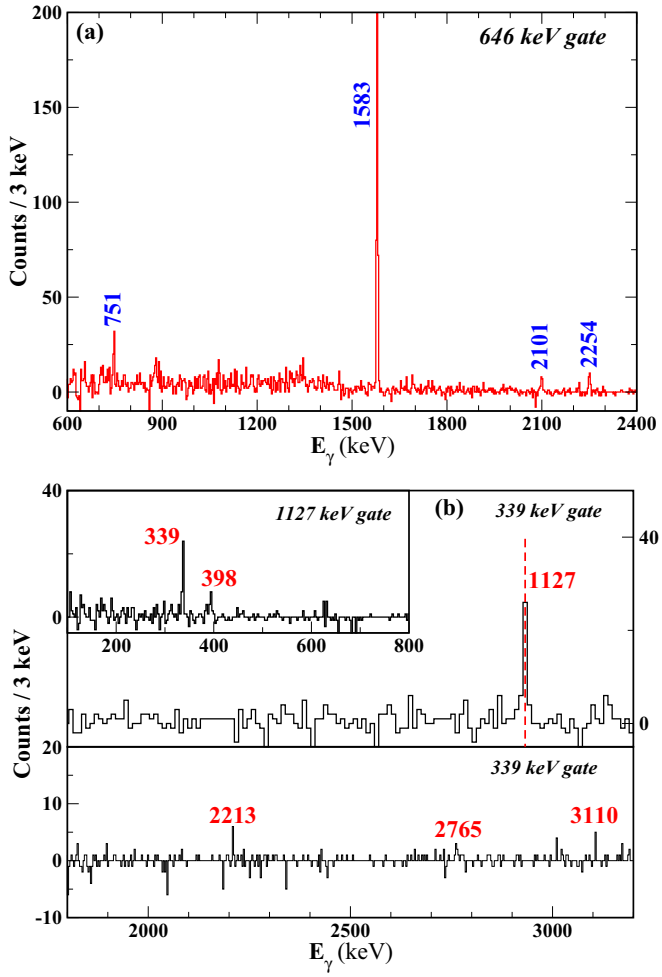

FIG. 11. (a) and (b) Coincidences observed for the transitions that are proposed to be in ^{37}S and ^{39}S, respectively. See the text for more details.

parent nucleus has a $J^\pi = 1/2^+$. A tentative log ft of 4.70(8) has been assigned to that state.

For ^{39}P decay to ^{39}S, the 1127-keV transition is shown to be in coincidence with the 339- and 398-keV transitions [Fig. 11(b)]. The 339- and 398-keV transitions do not show any coincidence and, thus, are proposed to deexcite the 398-keV state as was suggested in previous in-beam studies [25,26]. Thus, a level at 1525 keV is placed which also has a 1525-keV transition in parallel going directly to the ground state. The same γ transitions were observed by Winger *et al.* [24]. Furthermore, in the 339-keV gate, we observe weak coincidences with transitions at 2213, 2765, and 3110 keV not reported by Ref. [24]. The proposed level scheme for ^{39}S shown in Fig. 12 shows these new levels at 2611(2), 3163(3), and 3309(3) keV. The two strongest γ transitions in the decay are the 1525 keV [100(7)%] and 1127 keV [48(4)%] which deexcite the level at 1525 keV. Strong feeding to this state suggests allowed GT decay limiting its spin to $1/2^+$, $3/2^+$. A 466-keV transition previously proposed in ^{39}S based on the β-delayed neutron emission from ^{40}P [27] was not observed in this study.

IV. DISCUSSION

In this paper, we have reported the β^- decay of neutron-rich odd-A nuclei, namely, ^{37}Al, ^{37,39}Si, ^{37,39}P to populate excited states in the daughter nuclei. In all the pairs studied, the parent and daughter nuclei have opposite ground-state parities, and hence, the β^- decay populate excited states in the daughter of parity opposite to the ground state, i.e., $1p1h$ states *via* allowed GT transitions. However, there are quite some differences in the decay of these nuclei mainly in the distribution of the GT strength. In a recent publication by Yoshida *et al.* [11], it was calculated that the low-lying GT strengths of even-even nuclei are considerably larger than those of the neighboring odd-A and odd-odd nuclei. It was proposed that this even-odd effect is caused by the $J^\pi = 1^+$ proton-neutron pairing interaction which causes the 1^+ states to occur low in energy in the odd-odd daughter nuclei. They defined a strong low-energy GT transition as the one to a discrete level below $E^* = 5$ MeV that has a log $ft < 4.58$ [or B(GT) > 0.10].

In the current paper, no state with a log ft value less than 4.58 was observed. However, in our earlier work on the β^- decay of ^{38,40}Si, following the above definition, strong low-energy GT transitions were found as can be seen in Fig. 13 [5]. In both cases, 1^+ states were identified in ^{38,40}P at around 2 MeV confirming the proposition of Ref. [11]. The clear contrast to the decay of the neighboring odd-A ^{37,39}Si, presented in this paper, highlights the odd-even dependence. However, we see further differences even in the decay of odd-A nuclei depending on whether the daughter nucleus has an odd proton or an odd neutron. When the daughter has an odd neutron along with a paired proton, the $1p1h$ state has a large overlap with the parent ground state leading to strong β^- decay to the $1p1h$ state. This is illustrated schematically by taking the example of decay of ^{37}Al, ^{37}Si, and ^{37}P in Fig. 14 where we show the dominant neutron and proton configurations of the parent ground state (top) and the $1p1h$ states populated in the daughter (bottom). For ^{37}Al, the dominant decay will be the conversion: $\nu d_{3/2}$ to $\pi d_{5/2}$ creating a $3/2^+$ state in ^{37}Si which is the state populated predominantly (Fig. 3). On the contrary, when ^{37}Si decays, the $\nu d_{3/2}$ to $\pi d_{3/2}$ conversion will leave three holes which can couple in many ways leading to a number of states which can be populated in the β^- decay.

Configuration interaction shell-model calculations with the SDPFSDG-MU interaction [11] were performed both for the $0p0h$ and for the $1p1h$ states in the full sd-fp-sdg valence space to interpret the results. The $sd + pf$ shell component is exactly the same as the SDPF-MU interaction [10,28], and the remaining two-body matrix elements are obtained from a version of the $V_{\rm MU}$ interaction [29] that is adopted in the SDPF-MU interaction. The single-particle energies and two-body matrix elements used in the SDPF-MU calculations are based on existing interactions: USD [30] for the sd shell and GXPF1B [31] for the fp shell. The sd-fp cross-shell interaction is given by a monopole-based universal interaction $V_{\rm MU}$ [29]. The $V_{\rm MU}$ includes the tensor force and embodies shell evolution, i.e., the displacement of single-particle orbitals with neutron excess. To compare theoretical B(GT)

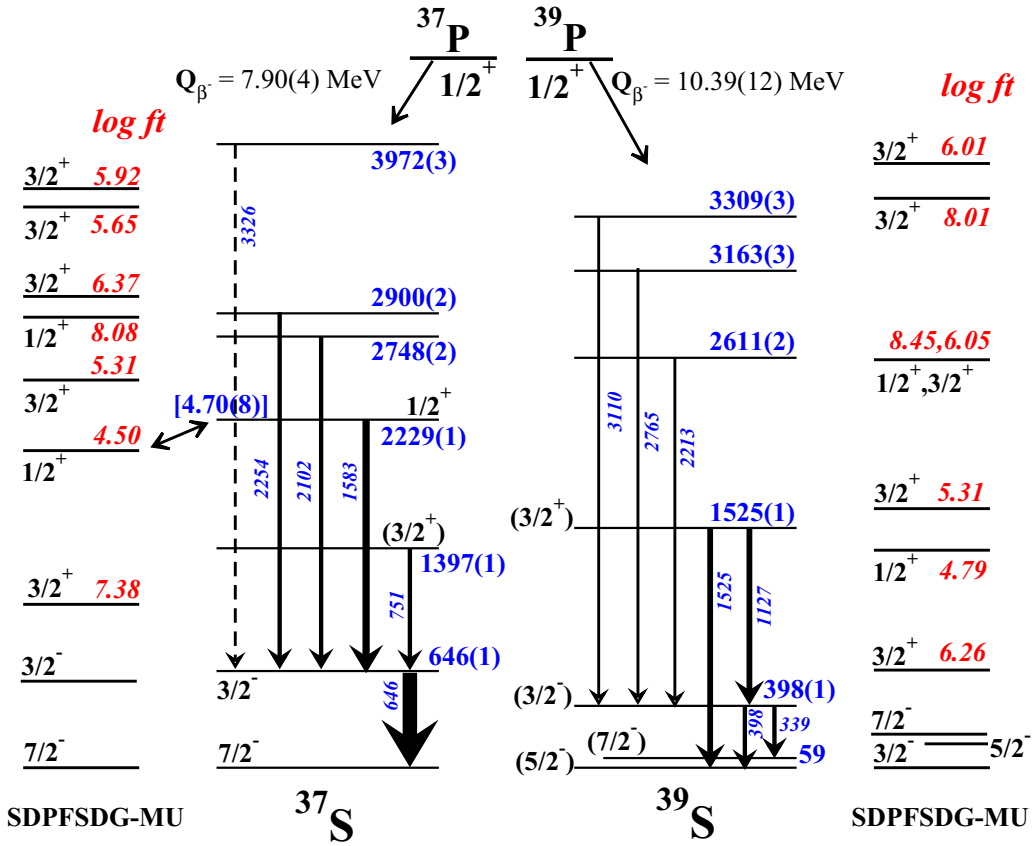

FIG. 12. Partial level scheme of ^{37,39}S as established in the present β^- decay study of ^{37,39}P along with shell-model calculations using the SDPFSDG-MU interaction. Positive-parity $1p1h$ states with spins of $1/2$ and $3/2$ only are shown for the SM calculations.

values to experimental values, a quenching factor of $q = 0.74$ was used in the shell-model calculations.

For the ^{37}Al decay as shown in Fig. 3, the β^- decay strongly populates the state at 717 keV in ^{37}Si with ∼31% of the feeding going to the one state. Using the measured $T_{1/2}$ and Q_{β^-} [17] a log ft value of 4.72(3) was calculated for that

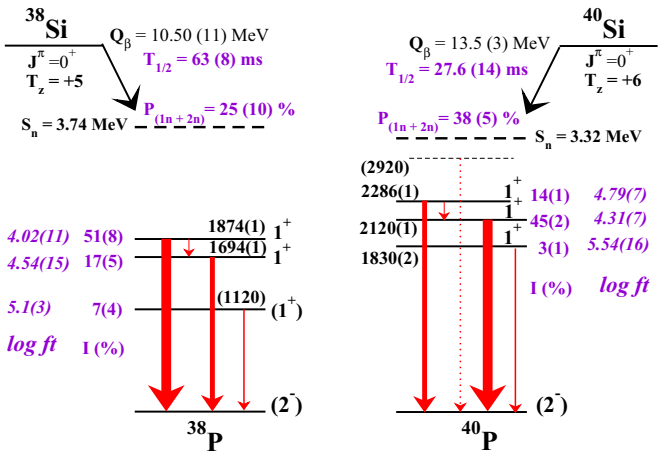

FIG. 13. Partial level scheme of ^{38,40}P as established in the β^- decay of ^{38,40}Si from Ref. [5]. A tentative 2940-keV state has been added not shown in Ref. [5].

state which classifies it as an allowed decay. Decaying from the $5/2^+$ ground state in ^{37}Al limits its J^π to $3/2^+$, $5/2^+$, or $7/2^+$. It decays both to the ground state which is predicted to be $5/2^-$ and to the 156-keV state which is likely a $3/2^-$ state based on shell-model calculation. The shell model predicts a low-lying $3/2^+$ state at 550 keV with a log ft of 4.67, an excellent candidate for the experimentally observed state at 717 keV. The calculated $3/2^+$ state at 550 keV is a $1p1h$ state with a likely configuration of $\nu d_{3/2}^{-1} f_{7/2}^4$ suggesting a very small $N = 20$ gap or large correlation due to deformation. The experimental 1270-keV state with a log ft of 5.16(5) is an excellent candidate for the calculated $5/2^+$ state at 1570 keV consistent with its decay to the low-lying negative-parity states.

For the odd-A ^{37,39}Si isotopes, the β decay proceeds in a remarkably different fashion than for ^{37}Al as noted before. Inspecting Figs. 6 and 10, again it is clear that the allowed GT transitions from the $5/2^-$ ground state of these isotopes do not favor any single state in the daughter nuclei, rather the strength is fragmented. This would imply a very small overlap between the ground state of the Si isotopes and the negative-parity states in ^{37,39}P. The states in the shaded boxes near the top of both figures are proposed to be the negative-parity states in the spin range of 3/2 to 7/2.

The experimental level schemes of ^{37,39}P are compared to shell-model calculations in Fig. 15 along with

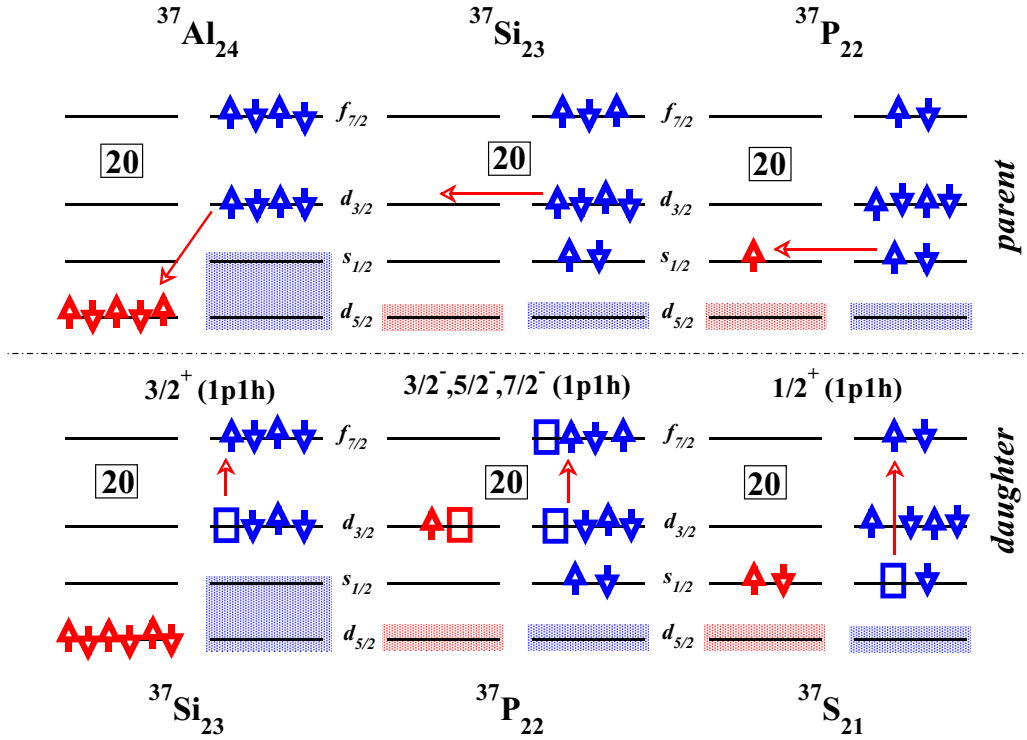

FIG. 14. Simplistic visualization of the β^- decay of ^{37}Al, ^{37}Si, and ^{37}P to show the dominant configuration of the parent ground state and the corresponding state that is created in the daughter nuclei. The shaded boxes represent filled orbitals. The solid boxes show the hole created in the β decay.

^{35}P ($N = 20$). The shell-model calculations predict a large number of negative-parity states [11], however, in the figure only five states of each spin 3/2, 5/2, and 7/2 which would be fed by allowed transitions are displayed for both ^{37,39}P. The density of states observed and calculated is in reasonable agreement between 3 and 5 MeV. Other spin states in this energy bin which would correspond to first forbidden decay have large predicted log ft values (>7.0) unlikely to be observed in the present experiment. For both ^{37,39}P, the negative-parity states appear above 3 MeV. It is noteworthy that, although both ^{37}Si and ^{39}P have the same neutron excess ($T_z = +9/2$) with one unit higher charge for P, the observed $1p1h$ states shift significantly higher from ≈700 keV in ^{37}Si to ≈3 MeV.

The calculated states in ^{37,39}P mostly have log ft values higher than 5 with no strong branch or a small log ft for any state (see Table II). This can explain the fragmented GT strength seen for ^{37,39}Si decay. The lowest $7/2^-$ states for ^{37,39}P are calculated to be at 3.033 and 3.097 MeV, respectively, with log ft values of 6.21 and 6.06. This is in contrast with the lighter ^{35}P isotope where, in the β^- decay of ^{35}Si, the tentative first $7/2^-$ state has a large branch shown by the small log ft value in Fig. 15. This is reproduced well by the calculation with the first and second $7/2^-$ states at 3.456 and 4.093 MeV having log ft of 5.08 and 4.58,, respectively.

Although the agreement between the experimentally proposed negative-parity $1p1h$ states and the shell-model predictions in ^{37,39}P is rather qualitative, on the other hand, the low-lying positive-parity states ($0p0h$) show good agreement. These states are fed indirectly by the decay of high-lying states. For ^{37}P, the shell-model calculation suggests that the 2200- and 2664-keV levels are the second $3/2^+$ and $5/2^+$ states, respectively. These levels can decay both to the $3/2^+_1$ and $5/2^+_1$ states at 861 and 1300 keV, respectively, consistent with the data. The 2481-keV state has been previously tentatively assigned ($9/2^+$) based on its decay to the $5/2^+_1$ state, however, comparison with the calculations suggest that both $7/2^+$ and $9/2^+$ are likely. For ^{39}P, the 1599-keV state can be identified with the predicted $7/2^+_1$ state with a decay branch to only the $3/2^+$ state at 355 keV. The previous assignment of $9/2^+$ to the 2173-keV state is consistent with the present experiment. The close-by state at 2192 keV could be the second $5/2^+$ state predicted at 2495 keV with decays to both the $3/2^+_1$ and the $5/2^+_1$ states at 355 and 973 keV, respectively, similar to ^{37}P.

The systematics of the lowest-energy states of $J^\pi = 3/2^+$, $5/2^+$, $7/2^+$, and $9/2^+$ are shown in Fig. 16(a) for ^{35,37,39}P. As is evident from the figure, all these states drop rather rapidly when two neutrons are added to $N = 20$, suggesting that they do not have a predominantly single-particle structure anymore. They continue to fall in energy as more neutrons are added. This trend had already been pointed out in previous studies for the $3/2^+$ and $5/2^+$ states [32,33], and from the present paper, we can say that the trend is similar for the $7/2^+$ and $9/2^+$ states too. The compression of the spectrum is suggestive of deformation in this region ($N \sim 28$ for $Z = 12$–16) driven by the narrowing $N = 28$ shell gap and the near degeneracy of the $\pi d_{3/2}$ and $\pi s_{1/2}$ orbitals. The development of deformation for $N > 20$ is also reflected in the systematic of half-lives of Si isotopes as shown in Fig. 16(b) where again a sudden drop is observed beyond $N = 20$.

TABLE II. Results of shell-model calculations using the SDPFSDG-MU interaction (excitation energies in MeV and corresponding log ft values) for the states in odd-even $^{35-39}$P expected to be populated in the β decay. The ground states of parent isotopes ^{35,37,39}Si are assumed to be $7/2^-$, $5/2^-$, and $5/2^-$, respectively, whereas all the odd-A P isotopes have a $1/2^+$ ground state.

Isotope	J_n^π	SDPFSDG-MU		Isotope	J_n^π	SDPFSDG-MU		Isotope	J_n^π	SDPFSDG-MU	
		E^*	log ft			E^*	log ft			E^*	log ft
^{35}P	$\frac{5}{2}^-_1$	4.444	5.57	^{37}P	$\frac{3}{2}^-_1$	3.626	5.86	^{39}P	$\frac{3}{2}^-_1$	3.452	5.15
	$\frac{5}{2}^-_2$	4.583	5.59		$\frac{3}{2}^-_2$	3.770	5.77		$\frac{3}{2}^-_2$	3.781	5.68
	$\frac{5}{2}^-_3$	4.971	4.71		$\frac{3}{2}^-_3$	4.154	5.18		$\frac{3}{2}^-_3$	3.892	6.76
	$\frac{5}{2}^-_4$	5.157	5.49		$\frac{3}{2}^-_4$	4.210	6.66		$\frac{3}{2}^-_4$	4.084	6.29
	$\frac{5}{2}^-_5$	5.467	5.00		$\frac{3}{2}^-_5$	4.224	5.10		$\frac{3}{2}^-_5$	4.240	5.47
	$\frac{7}{2}^-_1$	3.456	5.08		$\frac{5}{2}^-_1$	3.410	6.53		$\frac{5}{2}^-_1$	3.623	8.35
	$\frac{7}{2}^-_2$	4.093	4.58		$\frac{5}{2}^-_2$	3.568	5.07		$\frac{5}{2}^-_2$	3.707	5.79
	$\frac{7}{2}^-_3$	4.593	5.94		$\frac{5}{2}^-_3$	3.673	6.47		$\frac{5}{2}^-_3$	3.947	4.83
	$\frac{7}{2}^-_4$	5.169	5.10		$\frac{5}{2}^-_4$	4.042	4.79		$\frac{5}{2}^-_4$	4.186	6.02
	$\frac{7}{2}^-_5$	5.815	5.77		$\frac{5}{2}^-_5$	4.143	5.62		$\frac{5}{2}^-_5$	4.224	6.14
	$\frac{9}{2}^-_1$	3.850	6.03		$\frac{7}{2}^-_1$	3.033	6.21		$\frac{7}{2}^-_1$	3.097	6.06
	$\frac{9}{2}^-_2$	4.462	5.80		$\frac{7}{2}^-_2$	3.524	5.96		$\frac{7}{2}^-_2$	3.707	6.73
	$\frac{9}{2}^-_3$	5.829	4.34		$\frac{7}{2}^-_3$	3.846	6.14		$\frac{7}{2}^-_3$	3.934	6.83
	$\frac{9}{2}^-_4$	6.137	4.49		$\frac{7}{2}^-_4$	3.891	7.12		$\frac{7}{2}^-_4$	4.135	6.53
	$\frac{9}{2}^-_5$	6.501	6.39		$\frac{7}{2}^-_5$	4.193	5.50		$\frac{7}{2}^-_5$	4.331	5.15

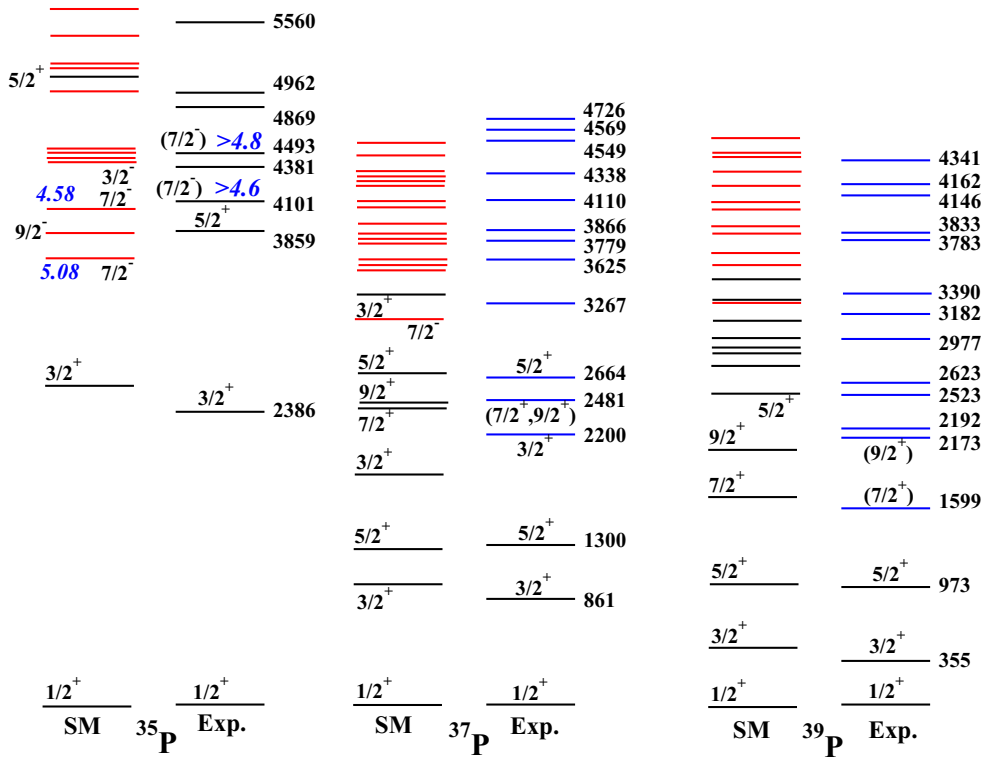

FIG. 15. Partial level scheme of ^{35,37,39}P compared to SM calculations using the SDPFSDG-MU interaction [10,11]. The experimental data for ^{35}P taken from NNDC [17]. For the calculations, black are positive-parity states whereas red are negative-parity states. For the experiment, shown in black are previously known states whereas blue are the new ones. The measured and calculated log ft for the $7/2^-$ states in ^{35}P (blue string) are also indicated.

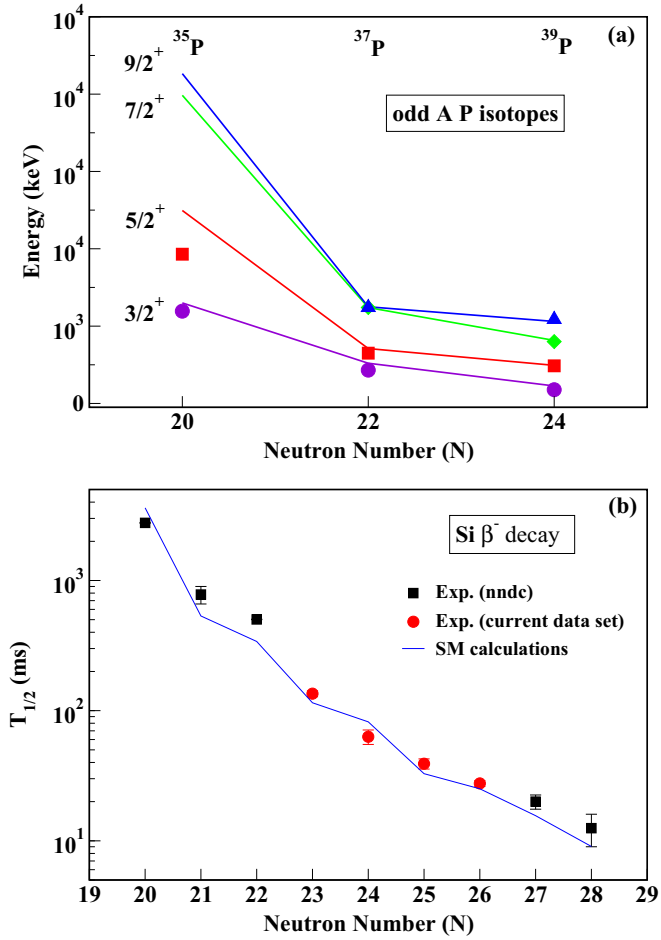

FIG. 16. (a) Systematics of low-lying positive-parity states in ^{35,37,39}P. The solid lines represent shell-model calculations using the SDPFSDG-MU interaction whereas experimental states are shown by solid symbols. Data for ^{37,39}P is from the present paper whereas literature values for ^{35}P are from Ref. [17]. For ^{35}P, calculations were performed in the *sd*-model space, hence, the overprediction of the $5/2^+$ state. (b) Measured half-lives of Si isotopes with $N = 20$ to $N = 28$ (solid symbols) along with the SDPFSDG-MU predictions (solid line). The experimental points in red are from the current data set. The half-lives of ^{38,40}Si were previously reported in Ref. [5] whereas the black points are from Refs. [17,18].

Further down the decay chain, the levels in ^{37,39}S populated in the decay of ^{37,39}P decay were shown in Fig. 12 along with the predictions of the shell-model calculations for the $1p1h$ states using the SDPFSDG-MU interaction. In ^{37}S, the state at 2229(1) keV decaying by the strong 1583-keV γ transition can be identified with the calculated $1/2^+_1$ state based on good energy agreement and small log ft values. As evident from Fig. 11, the other states in ^{37}S are very weakly populated and are good candidates for the $3/2^+$ states predicted with much larger log ft values. The ground state of ^{37}S with $N = 21$ has a J^π of $7/2^-$, and hence, none of the states observed with likely spins of $1/2^+$ and $3/2^+$ are expected to decay to it.

In the case of ^{39}S, the 1525(1)-keV state is fed with strong β branching and, thus, should be either a $1/2^+$ or a $3/2^+$ state (allowed GT decay). It has strong decay branches to the ground state as well as to the 398(1)-keV state. In previous in-beam studies of ^{39}S, the 398(1)-keV state is proposed to have $J^\pi = 3/2^-$. The ground-state configuration of even-Z $N = 23$ isotopes in a simple shell-model picture is described in terms of the coupling of the three extra $f_{7/2}$ neutrons to an inert proton core. In some cases (e.g., deformed nuclei), the lowest state of such a $(j)^3$ configuration has a total angular momentum different from $J = j$ as a result of residual interactions. For example, the ground-state spin and parity of ^{37}Si is $5/2^-$. The adopted ground-state J^π value of $7/2^-$ for ^{39}S is based on systematic [34], however, no model-independent assignment has been performed so far. The decay of the proposed low spin 1525(1)-keV state to the ground state in the present paper strongly suggests $5/2^-$. With strong decays to the $5/2^-$ and the $3/2^-$ states, the 1525(1)-keV state is more likely to be a $3/2^+$ state than a $1/2^+$. These tentative assignments are shown in Fig. 12. The shell-model calculations predict a ground-state triplet with spins $3/2^-, 5/2^-, 7/2^-$ within 200 keV consistent with the experimental observation. There is a $3/2^+$ state predicted at 1.65 MeV which could correspond to the experimentally observed state. The calculation also predicts a close-by $1/2^+$ state at 1.39 MeV with a small log ft which is not seen experimentally. The $3/2^+$ states above 2 MeV are predicted to be weakly populated and will correspond well with the observed states at 2611, 3163, and 3309 keV.

V. SUMMARY AND CONCLUSIONS

The β^- decay of exotic nuclides ^{37}Al and ^{39}Si both with $T_z = +11/2$ was studied at the National Superconducting Cyclotron Laboratory. This allowed us to establish the first elaborate level schemes of ^{37}P and ^{39}P. Tentative J^π assignments were made to several low-lying positive-parity states in both P isotopes, whereas negative-parity states populated by the β^- decay were identified for the first time. The level scheme of ^{37}Al as established from the current data is consistent with a recent study with the addition of precise log ft values for the populated states. The level schemes of ^{37}S and ^{39}S following β decay are also proposed based on new coincidences that could be observed in this paper. Shell-model calculations using the SDPFSDG-MU interaction successfully described the level structure in these exotic nuclei. We have also obtained more precise β-decay half-lives of ^{37}Si and ^{39}Si.

It proved instructive to compare the distribution of β-decay strength for the various isotopes studied in the paper along with some of our previous results from the same data set. There was a clear odd-even pattern observed, whereby the even-A nuclei, such as ^{38}Si and ^{40}Si preferentially populate low-lying states with small values of log ft in the daughter, whereas, in the neighboring odd-A isotopes, the β-decay strength is completely fragmented. Our observations strongly corroborate the recent predictions of Yoshida *et al.* [11].

ACKNOWLEDGMENTS

The authors thank the NSCL operations staff for the excellent beam and support during the experiment. Help from A. O.

Macchiavelli during the experiment is also appreciated. The work was supported by NSF Grants No. PHY-1401574 (FSU) and No. PHY-1102511 (NSCL), U.S. Department of Energy under Contracts No. DEAC02-05CH11231 (LBNL) and No. DE-SC0009883 (FSU), and the U.S. National Nuclear Security Agency under Awards No. DE-NA0000979, No. DE-NA0002132, No. DE-NA0003221, and No. DE-NA0003180. Some authors want to acknowledge support from JSPS KAKENHI (Japan), Grants No. 25870168, No. 15K05094, and No. 17J06775.

[1] B. Rubio and W. Gelletly, Beta decay of exotic nuclei, in *The Euroschool Lectures on Physics with Exotic Beams, Vol. III*, edited by J. S. Al-Khalili and E. Roeckl, Lecture Notes in Physics, Vol. 764 (Springer-Verlag, Berlin, Heidelberg, 2009), pp. 99–151, 1st ed.

[2] W. Loveland, D. J. Morrissey, and G. T. Seaborg, *Modern Nuclear Chemistry* (John Wiley & Sons Inc., Hoboken, NJ, 2006).

[3] M. Madurga, S. V. Paulauskas, R. Grzywacz, D. Miller, D. W. Bardayan, J. C. Batchelder, N. T. Brewer, J. A. Cizewski, A. Fijałkowska, C. J. Gross, M. E. Howard, S. V. Ilyushkin, B. Manning, M. Matoš, A. J. Mendez II, K. Miernik, S. W. Padgett, W. A. Peters, B. C. Rasco, A. Ratkiewicz, K. P. Rykaczewski, D. W. Stracener, E. H. Wang, M. Wolińska-Cichocka, and E. F. Zganjar, Phys. Rev. Lett. **117**, 092502 (2016).

[4] M. F. Alshudifat, R. Grzywacz, M. Madurga, C. J. Gross, K. P. Rykaczewski, J. C. Batchelder, C. Bingham, I. N. Borzov, N. T. Brewer, L. Cartegni, A. Fijałkowska, J. H. Hamilton, J. K. Hwang, S. V. Ilyushkin, C. Jost, M. Karny, A. Korgul, W. Królas, S. H. Liu, C. Mazzocchi, A. J. Mendez II, K. Miernik, D. Miller, S. W. Padgett, S. V. Paulauskas, A. V. Ramayya, D. W. Stracener, R. Surman, J. A. Winger, M. Wolińska-Cichocka, and E. F. Zganjar, Phys. Rev. C **93**, 044325 (2016).

[5] V. Tripathi, R. S. Lubna, B. Abromeit, H. L. Crawford, S. N. Liddick, Y. Utsuno, P. C. Bender, B. P. Crider, R. Dungan, P. Fallon, K. Kravvaris, N. Larson, A. O. Macchiavelli, T. Otsuka, C. J. Prokop, A. L. Richard, N. Shimizu, S. L. Tabor, A. Volya, and S. Yoshida, Phys. Rev. C **95**, 024308 (2017).

[6] A. Gottardo, D. Verney, I. Deloncle, S. Péru, C. Delafosse, S. Roccia, I. Matea, C. Sotty, C. Andreoiu, C. Costache, M.-C. Delattre, A. Etilé, S. Franchoo, C. Gaulard, J. Guillot, F. Ibrahim, M. Lebois, M. MacCormick, N. Marginean, R. Marginean, M. Martini, C. Mihai, I. Mitu, L. Olivier, C. Portail, L. Qi, B. Roussière, L. Stan, D. Testov, J. Wilson, and D. T. Yordanov, Phys. Lett. B **772**, 359 (2017).

[7] K. Steiger, S. Nishimura, Z. Li, R. Gernhäuser, Y. Utsuno, R. Chen, T. Faestermann, C. Hinke, R. Krücken, M. Kurata-Nishimura, G. Lorusso, Y. Miyashita, N. Shimizu, K. Sugimoto, T. Sumikama, H. Watanabe, and K. Yoshinaga, Eur. Phys. J. A **51**, 117 (2015).

[8] A. Hodsdon, R. Chapman, X. Liang, F. Haas, J. Ollier, E. Caurier, F. Nowacki, M.-D. Salsac, F. Azaiez, S. Beghini, B. Behera, M. Burns, L. Corradi, D. Curien, A. N. Deacon, Z. Dombrádi, E. Farnea, E. Fioretto, A. Gadea, A. Jungclaus, K. L. Keyes, A. Latina, N. Mărginean, G. Montagnoli, D. Napoli, D. O'Donnell, A. Papenberg, F. Scarlassara, J. F. Smith, K.-M. Spohr, M. Stanoiu, A. Stefanini, S. Szilner, M. Trotta, C. Ur, D. Verney, and Z. Wang, Phys. Rev. C **75**, 034313 (2007).

[9] O. Sorlin, Z. Dombrádi, D. Sohler, F. Azaiez, J. Timár, Y.-E. Penionzhkevich, F. Amorini, D. Baiborodin, A. Bauchet, F. Becker, M. Belleguic, C. Borcea, C. Bourgeois, Z. Dlouhy, C. Donzaud, J. Duprat, L. Gaudefroy, D. Guillemaud-Mueller, F. Ibrahim, M. J. Lopez, R. Lucas, S. M. Lukyanov, V. Maslov, J. Mrazek, C. Moore, F. Nowacki, F. Pougheon, M. G. Saint-Laurent, F. Sarazin, J. A. Scarpaci, G. Sletten, M. Stanoiu, C. Stodel, M. Taylor, and C. Theisen, Eur. Phys. J. A **22**, 173 (2004).

[10] Y. Utsuno, T. Otsuka, B. A. Brown, M. Honma, T. Mizusaki, and N. Shimizu, Phys. Rev. C **86**, 051301 (2012).

[11] S. Yoshida, Y. Utsuno, N. Shimizu, and T. Otsuka, Phys. Rev. C **97**, 054321 (2018).

[12] A. Gade and B. M. Sherrill, Phys. Scr. **91**, 053003 (2016).

[13] D. J. Morrissey *et al.*, Nucl. Instrum. Methods Phys. Res., Sect. B **204**, 90 (2003).

[14] N. Larson, S. Liddick, M. Bennett, A. Bowe, A. Chemey, C. Prokop, A. Simon, A. Spyrou, S. Suchyta, S. Quinn, S. Tabor, P. Tai, V. Tripathi, and J. VonMoss, Nucl. Instrum. Methods Phys. Res., Sect. A **727**, 59 (2013).

[15] W. Mueller, J. Church, T. Glasmacher, D. Gutknecht, G. Hackman, P. Hansen, Z. Hu, K. Miller, and P. Quirin, Nucl. Instrum. Methods Phys. Res., Sect. A **466**, 492 (2001).

[16] V. Tripathi, S. L. Tabor, C. R. Hoffman, M. Wiedeking, A. Volya, P. F. Mantica, A. D. Davies, S. N. Liddick, W. F. Mueller, A. Stolz, B. E. Tomlin, T. Otsuka, and Y. Utsuno, Phys. Rev. C **73**, 054303 (2006).

[17] ENSDF database, http://www.nndc.bnl.gov/ensdf/.

[18] R. Han, X. Q. Li, W. G. Jiang, Z. H. Li, H. Hua, S. Q. Zhang, C. X. Yuan, D. X. Jiang, Y. L. Ye, J. Li, Z. H. Li, F. R. Xu, Q. B. Chen, J. Meng, J. S. Wang, C. Xu, Y. L. Sun, C. G. Wang, H. Y. Wu, C. Y. Niu, C. G. Li, C. He, W. Jiang, P. J. Li, H. L. Zang, J. Feng, S. D. Chen, Q. Liu, X. C. Chen, H. S. Xu, Z. G. Hu, Y. Y. Yang, P. Ma, J. B. Ma, S. L. Jin, Z. Bai, M. R. Huang, Y. J. Zhou, W. H. Ma, Y. Li, X. H. Zhou, Y. H. Zhang, G. Q. Xiao, and W. L. Zhan, Phys. Lett. B **772**, 529 (2017).

[19] http://www.nndc.bnl.gov/logft/.

[20] J. P. Dufour, R. Del Moral, A. Fleury, F. Hubert, D. Jean, M. S. Pravikoff, H. Delagrange, H. Geissel, and K.-H. Schmidt, Z. Phys. A - At. Nucl. **324**, 487 (1986).

[21] K. Yoneda, H. Sakurai, N. Aoi, N. Fukuda, T. Gomi, E. Ideguchi, N. Imai, H. Iwasaki, T. Kubo, Z. Liu, S. M. Lukyanov, T. Nakamura, M. Notani, H. Ogawa, Y. E. Penionzhkevich, W.-D. Schmidt-Ott, S. Shimoura, E. Sokol, Y. X. Watanabe, A. Yoshida, X. Zhou, and M. Ishihara, RIKEN Report No. RIKEN-98, 1999, p. 78.

[22] J. C. Hardy, L. C. Carraz, B. Jonson, and P. G. Hansen, Phys. Lett. B **71**, 307 (1977).

[23] R. Chapman, A. Hodsdon, M. Bouhelal, F. Haas, X. Liang, F. Azaiez, Z. M. Wang, B. R. Behera, M. Burns, E. Caurier, L. Corradi, D. Curien, A. N. Deacon, Z. Dombrádi, E. Farnea, E. Fioretto, A. Gadea, F. Ibrahim, A. Jungclaus, K. Keyes, V. Kumar, S. Lunardi, N. Marginean, G. Montagnoli, D. R. Napoli, F. Nowacki, J. Ollier, D. O'Donnell, A. Papenberg, G. Pollarolo, M.-D. Salsac, F. Scarlassara, J. F. Smith, K. M.

Spohr, M. Stanoiu, A. M. Stefanini, S. Szilner, M. Trotta, and D. Verney, Phys. Rev. C **92**, 044308 (2015).

[24] J. A. Winger, H. H. Yousif, W. C. Ma, V. Ravikumar, W. Lui, S. K. Phillips, R. B. Piercey, P. F. Mantica, B. Pritychenko, R. M. Ronningen, and M. Steiner, in *Exotic Nuclei and Atomic Masses (ENAM 98)*, edited by B. M. Sherrill, AIP Conf. Proc. No. 455 (AIP, Melville, New York, 1998), p. 606.

[25] R. Chapman, Z. M. Wang, M. Bouhelal, F. Haas, X. Liang, F. Azaiez, B. R. Behera, M. Burns, E. Caurier, L. Corradi, D. Curien, A. N. Deacon, Z. Dombrádi, E. Farnea, E. Fioretto, A. Gadea, A. Hodsdon, F. Ibrahim, A. Jungclaus, K. Keyes, V. Kumar, S. Lunardi, N. Mărginean, G. Montagnoli, D. R. Napoli, F. Nowacki, J. Ollier, D. O'Donnell, A. Papenberg, G. Pollarolo, M.-D. Salsac, F. Scarlassara, J. F. Smith, K. M. Spohr, M. Stanoiu, A. M. Stefanini, S. Szilner, M. Trotta, and D. Verney, Phys. Rev. C **94**, 024325 (2016).

[26] E. Lunderberg, A. Gade, V. Bader, T. Baugher, D. Bazin, J. S. Berryman, B. A. Brown, D. J. Hartley, F. Recchia, S. R. Stroberg, D. Weisshaar, and K. Wimmer, Phys. Rev. C **94**, 064327 (2016).

[27] J. A. Winger, P. F. Mantica, R. M. Ronningen, and M. A. Caprio, Phys. Rev. C **64**, 064318 (2001).

[28] Y. Utsuno, T. Otsuka, B. A. Brown, M. Honma, T. Mizusaki, and N. Shimizu, Prog. Theor. Phys. Suppl. **196**, 304 (2012).

[29] T. Otsuka, T. Suzuki, M. Honma, Y. Utsuno, N. Tsunoda, K. Tsukiyama, and M. Hjorth-Jensen, Phys. Rev. Lett. **104**, 012501 (2010).

[30] B. A. Brown and B. H. Wildenthal, Annu. Rev. Nucl. Part. Sci. **38**, 29 (1988).

[31] M. Honma, T. Otsuka, B. A. Brown, and T. Mizusaki, Eur. Phys. J. A **25**, 499 (2005).

[32] F. Nowacki and A. Poves, Phys. Rev. C **79**, 014310 (2009).

[33] A. Gade, B. A. Brown, D. Bazin, C. M. Campbell, J. A. Church, D. C. Dinca, J. Enders, T. Glasmacher, M. Horoi, Z. Hu, K. W. Kemper, W. F. Mueller, T. Otsuka, L. A. Riley, B. T. Roeder, T. Suzuki, J. R. Terry, K. L. Yurkewicz, and H. Zwahlen, Phys. Rev. C **74**, 034322 (2006).

[34] B. Singh and J. A. Cameron, Nucl. Data Sheets **107**, 225 (2006).